Appl Phys B (2009) 96: 509–516
DOI 10.1007/s00340-009-3483-2

Applied Physics B
Lasers and Optics

Vectorial partially coherent flat-topped beams and their nonparaxial propagation

Z. Mei · D. Zhao · G. Juguan

Received: 4 December 2008 / Revised version: 10 February 2009 / Published online: 3 April 2009

Abstract The concept of vectorial partially coherent flat-topped beams is proposed, and their nonparaxial propagation in free space is studied in detail. Based on the vector Rayleigh diffraction integral formulae, the analytical propagation expressions for the cross-spectral density matrix of the polarized vectorial nonparaxial partially coherent flat-topped beams are derived and applied to study the nonparaxial propagation properties of vectorial partially coherent flat-topped beams. The effect of propagation parameters on the intensity and the coherence property of the nonparaxial vectorial partially coherent flat-topped beam is illustrated and analyzed comparatively with the corresponding paraxial results.

PACS 41.85.Ew · 42.60.Jf · 42.25.Kb

1 Introduction

Laser beams with flat-topped spatial profiles have been widely investigated both theoretically and experimentally due to their wide applications in material thermal processing, inertial confinement fusion and otherwise. Several theoretical models have been proposed to describe light beams with flat-topped profiles, such as the super-Gaussian beam, the flattened Gaussian beam proposed by Gori, etc. [1, 2]. Recently, Li proposed a new theoretical model to describe the light beams with flat-topped profiles, which can be expressed as a finite series of lower-order Gaussian modes with different parameters [3]. Some extensive studies based on this model have been done on its propagation properties [4–6], yet those works have been limited mainly to the fully spatially coherent case. In practice, most light beams are partially coherent; completely coherent and completely incoherent beams are nonexistent. Recently, more and more attention has been paid to partially coherent beams with flat-topped profiles under the framework of the paraxial approximation [7–13]. However, the paraxial approximation is not applicable to beams with a large divergence angle or a small spot size that is comparable with the wavelength [14]. Therefore, it is necessary to consider partially coherent flat-topped beams and their nonparaxial propagation properties. The aim of this paper is to introduce vectorial partially coherent flat-topped beams and apply a 3×3 electric cross-spectral density matrix to investigate their nonparaxial propagation properties.

Z. Mei (✉) · G. Juguan
Department of Physics, Huzhou Teachers College, Huzhou 313000, China
e-mail: meizhangrong@yahoo.com

D. Zhao
Department of Physics, Zhejiang University, Hangzhou 310027, China

2 Theoretical analyses

For a quasi-monochromatic partially coherent beam generated by a source located in the plane $z = 0$ and propagating into the positive direction of the z-axis, the second-order coherence properties of such a vector field at any pair of points $\mathbf{r}_1, \mathbf{r}_2$ can be characterized with the 3×3 electric cross-spectral density matrix [15]

$$\overleftrightarrow{W}(\mathbf{r}_1, \mathbf{r}_2) = \left[W_{ij}(\mathbf{r}_1, \mathbf{r}_2)\right] = \left[\left\langle E_i^*(\mathbf{r}_1) E_j(\mathbf{r}_2)\right\rangle\right] \quad (i, j = x, y, z). \tag{1}$$

Here the asterisk denotes the complex conjugate and the angular brackets stand for the ensemble average in the sense of coherence theory in the space-frequency domain. The angular frequency ω is suppressed for brevity. $E(\mathbf{r}) = E_x(\boldsymbol{\rho}, z)\mathbf{i} + E_y(\boldsymbol{\rho}, z)\mathbf{j} + E_z(\boldsymbol{\rho}, z)\mathbf{k}$ is the vector field in the half-space $z > 0$, where $\mathbf{i}$, $\mathbf{j}$ and $\mathbf{k}$ are unit vectors in the x-, y- and z-directions, respectively, and $\boldsymbol{\rho} = (x, y)$ is the transverse position vector in the z-plane. The propagation of each component of the vector beam can be treated by the use of the vector Rayleigh diffraction integral formulae [16–20]:

$$E_i(\boldsymbol{\rho}, z) = -\frac{1}{2\pi}\int\int E_i(\boldsymbol{\rho}_0, 0)\frac{\partial}{\partial z}\left[\frac{\exp(ikR)}{R}\right]\mathrm{d}^2\boldsymbol{\rho}_0 \quad (i = x, y), \tag{2a}$$

$$E_z(\boldsymbol{\rho}, z) = \frac{1}{2\pi}\left\{\int\int E_x(\boldsymbol{\rho}_0, 0)\frac{\partial}{\partial x}\left[\frac{\exp(ikR)}{R}\right] + E_y(\boldsymbol{\rho}_0, 0)\frac{\partial}{\partial y}\left[\frac{\exp(ikR)}{R}\right]\right\}\mathrm{d}^2\boldsymbol{\rho}_0, \tag{2b}$$

where $R = [(x - x_0)^2 + (y - y_0)^2 + z^2]^{1/2}$, k is the wave number related to the wavelength λ by $k = 2\pi/\lambda$, and $\boldsymbol{\rho}_0 = (x_0, y_0)$ is the transverse position vector in the plane $z = 0$. Equation (2) is a general method suited to describing propagation in the extreme nonparaxial regime $w_0 < \sqrt{2}\lambda$, which in particular enables us to find an analytical solution associated with a realistic Gaussian boundary condition, valid for propagation distances $z \geq w_0^2/2\lambda$ [20], where w_0 is the waist width. When $R \gg \lambda$, in (2), the partial derivative of the nucleus $\exp(ikR)/R$ on the variables x, y and z can be approximated as

$$\frac{\partial}{\partial\gamma}\left[\frac{\exp(ikR)}{R}\right] \approx \frac{ik(\gamma - \gamma_0)}{R^2}\exp(ikR), \quad \gamma = x, y, \tag{3}$$

$$\frac{\partial}{\partial z}\left[\frac{\exp(ikR)}{R}\right] \approx \frac{ikz}{R^2}\exp(ikR). \tag{4}$$

Using the above approximation and substituting from (2) into (1), the following expression for the elements $W_{ij}(\boldsymbol{\rho}_1, \boldsymbol{\rho}_2, z)$ of the cross-spectral density matrix of the vector field in the output plane can be calculated in terms of matrix element $W_{ij}^0(\boldsymbol{\rho}_{10}, \boldsymbol{\rho}_{20}, 0)$ in the source plane [17], i.e.,

$$W_{\alpha\beta}(\boldsymbol{\rho}_1, \boldsymbol{\rho}_2, z) = \left(\frac{z}{\lambda}\right)^2\int\int W_{\alpha\beta}^0(\boldsymbol{\rho}_{10}, \boldsymbol{\rho}_{20}, 0) \times \frac{\exp[ik(R_2 - R_1)]}{R_2^2 R_1^2}\mathrm{d}^2\boldsymbol{\rho}_{10}\,\mathrm{d}^2\boldsymbol{\rho}_{20} \quad (\alpha, \beta = x, y), \tag{5a}$$

$$W_{\gamma z}(\boldsymbol{\rho}_1, \boldsymbol{\rho}_2, z) = -\frac{z}{\lambda^2}\int\int\left[W_{\gamma x}^0(\boldsymbol{\rho}_{10}, \boldsymbol{\rho}_{20}, 0)(x_2 - x_{20}) + W_{\gamma y}^0(\boldsymbol{\rho}_{10}, \boldsymbol{\rho}_{20}, 0)(y_2 - y_{20})\right] \times \frac{\exp[ik(R_2 - R_1)]}{R_2^2 R_1^2}\mathrm{d}^2\boldsymbol{\rho}_{10}\,\mathrm{d}^2\boldsymbol{\rho}_{20} \quad (\gamma = x, y), \tag{5b}$$

$$W_{zz}(\boldsymbol{\rho}_1, \boldsymbol{\rho}_2, z) = \frac{1}{\lambda^2}\int\int\left[W_{xx}^0(\boldsymbol{\rho}_{10}, \boldsymbol{\rho}_{20}, 0)(x_1 - x_{10})(x_2 - x_{20}) + 2W_{xy}^0(\boldsymbol{\rho}_{10}, \boldsymbol{\rho}_{20}, 0)(x_1 - x_{10})(y_2 - y_{20}) + W_{yy}^0(\boldsymbol{\rho}_{10}, \boldsymbol{\rho}_{20}, 0)(y_1 - y_{10})(y_2 - y_{20})\right] \times \frac{\exp[ik(R_2 - R_1)]}{R_2^2 R_1^2}\mathrm{d}^2\boldsymbol{\rho}_{10}\,\mathrm{d}^2\boldsymbol{\rho}_{20}. \tag{5c}$$

In (5), the R_1 and R_2 can be approximately expanded into [17, 20]

$$R_m = r_m + \frac{x_{0m}^2 + y_{0m}^2 - 2x_m x_{0m} - 2y_m y_{0m}}{2r_m} \quad (m = 1, 2), \tag{6}$$

where $r_m = (x_m^2 + y_m^2 + z^2)^{1/2}$. From (5) we can obtain the cross-spectral density matrix of vectorial partially coherent beams in the premise of the known source field, and further can analyze their optical intensity and spectral degree of coherence.

Let us consider a polarized partially coherent flat-topped beam generated by a Schell-model source, whose cross-spectral density function at plane $z = 0$ can be expressed in the following form:

$$W_{\alpha\beta}^0(\boldsymbol{\rho}_{10}, \boldsymbol{\rho}_{20}, 0) = \begin{cases} \displaystyle\sum_{n_1=1}^{N}\sum_{n_2=1}^{N}\frac{(-1)^{n_1+n_2-2}}{N^2}\binom{N}{n_1}\binom{N}{n_2} \\ \quad \times \exp\left(-\dfrac{n_1\boldsymbol{\rho}_{10}^2 + n_2\boldsymbol{\rho}_{20}^2}{w_0^2}\right)\exp\left(-\dfrac{|\boldsymbol{\rho}_{10} - \boldsymbol{\rho}_{20}|^2}{2\sigma_0^2}\right), \\ 0, \quad \text{otherwise} \end{cases} \quad (\alpha = \beta = x) \tag{7}$$

where $\binom{N}{n}$ denotes a binomial coefficient, w_0 is the waist width of the Gaussian beam and σ_0 is the correlation length. N ($N = 1, 2, 3, \ldots$) is the beam order. The degree of flatness increases with an increase of N. When $N = 1$, (7) reduces to the cross-spectral density of a fundamental partially coherent Gaussian Schell-model beam.

Replacing R_m in the exponential term of (5) with (6), and that in other terms with r_m, and substituting (7) into (5), after performing tedious integral calculations, we obtain the nonparaxial propagation analytical formula of the cross-spectral density matrix for a vectorial partially coherent flat-topped beam in free space:

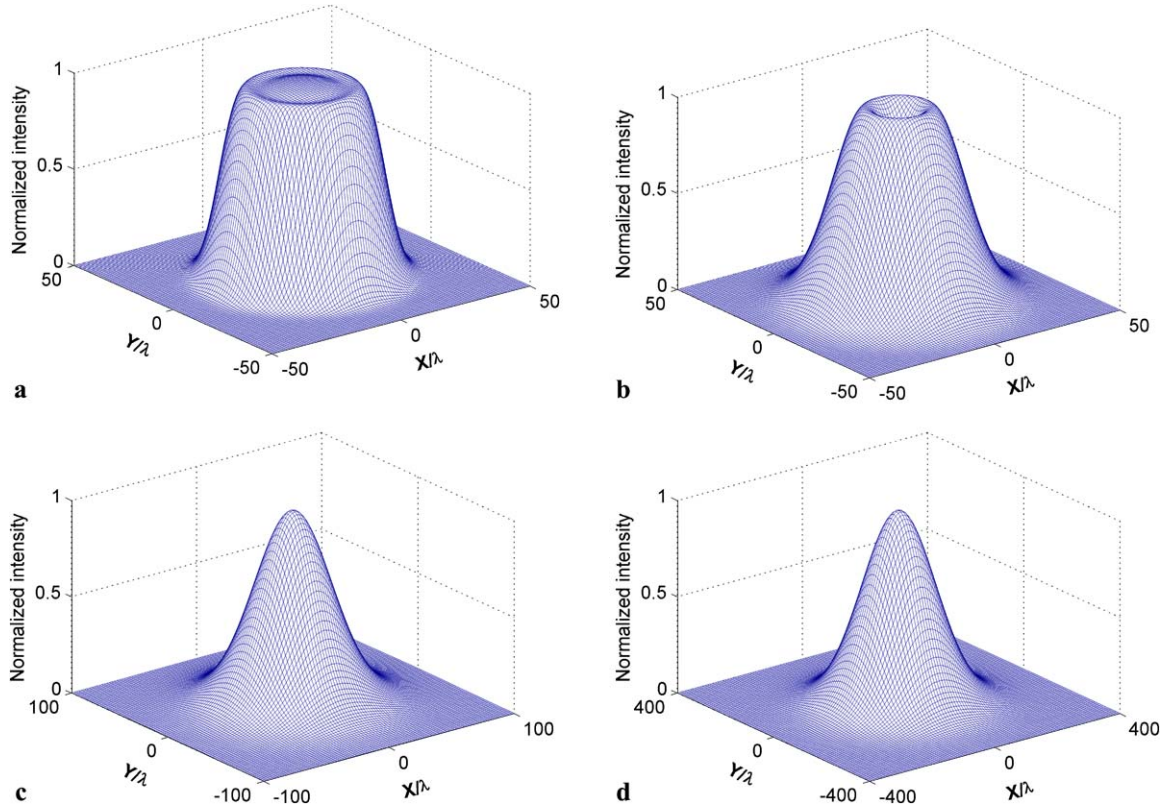

Fig. 1 Normalized three-dimensional irradiance distribution of a vectorial nonparaxial partially coherent flat-topped beam with $N = 20$ at various values of the propagation distances z. (**a**) $z = 0.1z_R$, (**b**) $z = 0.5z_R$, (**c**) $z = 5z_R$, (**d**) $z = 10z_R$

$$W_{xx}(\boldsymbol{\rho}_1, \boldsymbol{\rho}_2, z) = \sum_{n_1=1}^{N}\sum_{n_2=2}^{N} \frac{(-1)^{n_1+n_2-2}}{N^2}\binom{N}{n_1}\binom{N}{n_2} \times \frac{z^2 \exp[ik(r_2 - r_1)]}{r_1^2 r_2^2 P} \times \exp\left\{-\frac{k}{P}\left[C_1\frac{\boldsymbol{\rho}_2^2}{r_2^2} + C_2\frac{\boldsymbol{\rho}_1^2}{r_1^2} - \frac{kf_\sigma^2(x_1x_2 + y_1y_2)}{r_1r_2}\right]\right\}, \tag{8a}$$

$$W_{xz}(\boldsymbol{\rho}_1, \boldsymbol{\rho}_2, z) = \sum_{n_1=1}^{N}\sum_{n_2=2}^{N} \frac{(-1)^{n_1+n_2-2}}{N^2}\binom{N}{n_1}\binom{N}{n_2} \frac{z\exp[ik(r_2 - r_1)]}{r_1^2 r_2^2 P_1} \times \left\{\frac{2C_1}{P}\left[i\left(\frac{kf_\sigma^2 x_1}{2C_1 r_1} - \frac{x_2}{r_2}\right)\right] - x_2\right\} \times \exp\left\{-\frac{k}{P}\left[C_1\frac{\boldsymbol{\rho}_2^2}{r_2^2} + C_2\frac{\boldsymbol{\rho}_1^2}{r_1^2} - \frac{kf_\sigma^2(x_1x_2 + y_1y_2)}{r_1r_2}\right]\right\}, \tag{8b}$$

$$W_{zz}(\boldsymbol{\rho}_1, \boldsymbol{\rho}_2, z) = \sum_{n_1=1}^{N}\sum_{n_2=2}^{N} \frac{(-1)^{n_1+n_2-2}}{N^2}\binom{N}{n_1}\binom{N}{n_2} \frac{\exp[ik(r_2 - r_1)]}{r_1^2 r_2^2 P} \times \left[\left(1 - \frac{i}{2C_1 r_1}\right)x_1x_2 - \left(\frac{if_\sigma^2 kx_2}{P} + \frac{i2C_1x_1}{P} + \frac{x_1}{Pr_1}\right) \times \left(\frac{x_2}{r_2} - \frac{kf_\sigma^2 x_1}{2C_1 r_1}\right) - \frac{2C_1 kf_\sigma^2}{P^2}\left(\frac{x_2}{r_2} - \frac{kf_\sigma^2 x_1}{2C_1 r_1}\right)^2 + \frac{f_\sigma^2}{P}\right] \times \exp\left\{-\frac{k}{P}\left[C_1\frac{\boldsymbol{\rho}_2^2}{r_2^2} + C_2\frac{\boldsymbol{\rho}_1^2}{r_1^2} - \frac{kf_\sigma^2(x_1x_2 + y_1y_2)}{r_1r_2}\right]\right\}, \tag{8c}$$

and with the other matrix elements equal to zero. In (8),

$$C_1 = kf_\sigma^2/2 + n_1 kf_w^2 + i/2r_1, \tag{9}$$

$$C_2 = kf_\sigma^2/2 + n_2 kf_w^2 - i/2r_2, \tag{10}$$

$$P = 4C_1C_2 - k^2 f_\sigma^4, \tag{11}$$

where $f_w = 1/kw_0$ and $f_\sigma = 1/k\sigma_0$ are the key parameters for determining the nonparaxiality of the vectorial par-

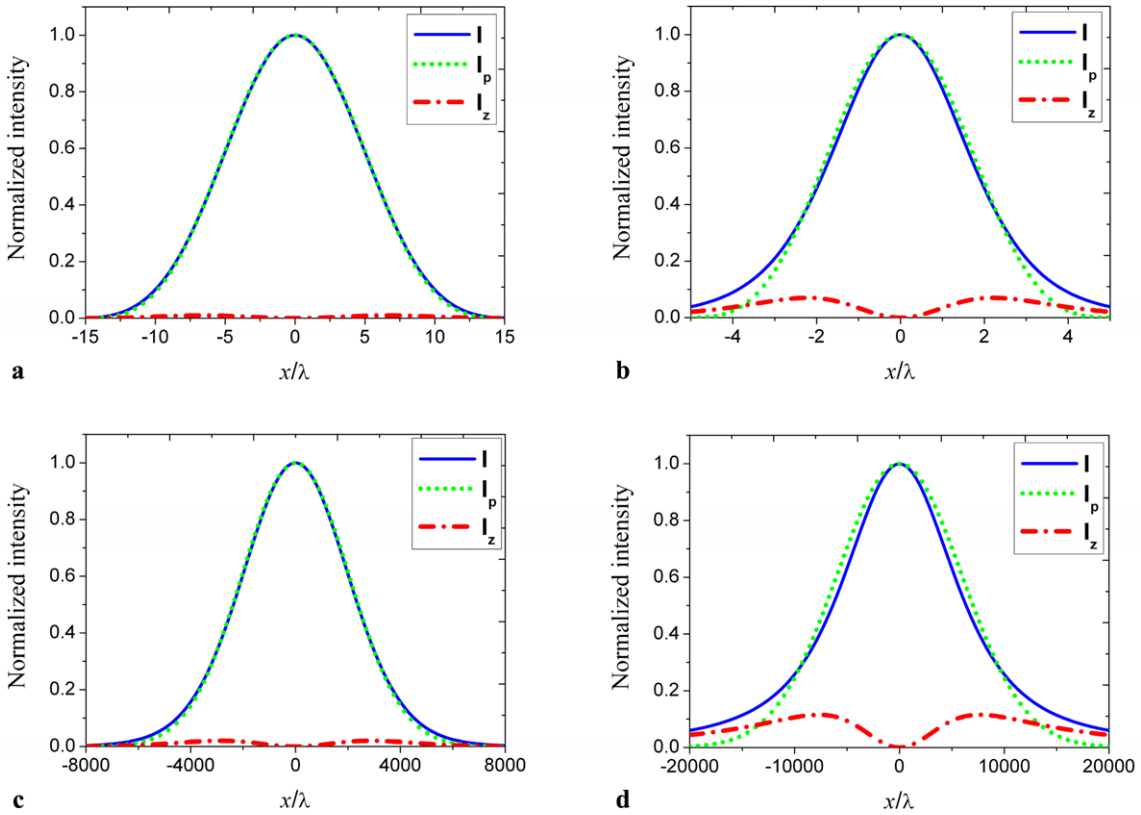

Fig. 2 Normalized irradiance distribution of a vectorial nonparaxial partially coherent flat-topped beam with $N = 20$ in the plane $z = 15z_R$ for different f_w and f_σ values. (**a**) $f_w = 0.17$, $f_\sigma = 0.01$; (**b**) $f_w = 0.5$, $f_\sigma = 0.01$; (**c**) $f_w = 0.01$, $f_\sigma = 0.17$; (**d**) $f_w = 0.01$, $f_\sigma = 0.5$

tially coherent flat-topped beam. According to [14], the parameter f_w must meet certain restrictive conditions. When $f_w \geq 1/\sqrt{2}$, a Gaussian beam loses its reality, and the paraxial approximation completely fails [14].

The intensity distribution of vectorial nonparaxial partially coherent flat-topped beams at the point $(\boldsymbol{\rho}, z)$ is given by the formula

$$I(\boldsymbol{\rho}, z) = \mathrm{Tr}\overleftrightarrow{W}(\boldsymbol{\rho}, \boldsymbol{\rho}, z) = W_{xx}(\boldsymbol{\rho}, \boldsymbol{\rho}, z) + W_{yy}(\boldsymbol{\rho}, \boldsymbol{\rho}, z) + W_{zz}(\boldsymbol{\rho}, \boldsymbol{\rho}, z). \quad (12)$$

The spectral degree of coherence of vectorial nonparaxial partially coherent flat-topped beams at a pair of points $r_1 = (\boldsymbol{\rho}_1, z)$ and $r_2 = (\boldsymbol{\rho}_2, z)$ is given by the formula

$$\mu(\boldsymbol{\rho}_1, \boldsymbol{\rho}_2, z) = \frac{\mathrm{Tr}\overleftrightarrow{W}(\boldsymbol{\rho}_1, \boldsymbol{\rho}_2, z)}{\sqrt{\mathrm{Tr}\overleftrightarrow{W}(\boldsymbol{\rho}_1, \boldsymbol{\rho}_1, z)}\sqrt{\mathrm{Tr}\overleftrightarrow{W}(\boldsymbol{\rho}_2, \boldsymbol{\rho}_2, z)}}, \quad (13)$$

where Tr stands for the trace of the matrix.

Within the paraxial regime, we often neglect the longitudinal component of the beam field and use the 2×2 cross-spectral density matrix to investigate the paraxial propagation properties of partially coherent beams. With the paraxial approximation $r_m \approx z + (x_m^2 + y_m^2)/2z$, (8) reduces to

$$W_p(\boldsymbol{\rho}_1, \boldsymbol{\rho}_2, z) = \sum_{n_1}^{N}\sum_{n_2}^{N} \frac{(-1)^{n_1+n_2-2}}{N^2}\binom{N}{n_1}\binom{N}{n_2} \times \frac{\exp[ik(\boldsymbol{\rho}_2^2 - \boldsymbol{\rho}_1^2)/2z]}{P'z^2} \times \exp\left\{-\frac{k}{P'z^2}\left[C_1'\boldsymbol{\rho}_2^2 + C_2'\boldsymbol{\rho}_1^2 - kf_\sigma^2(x_1x_2 + y_1y_2)\right]\right\}, \quad (14)$$

where

$$C_1' = kf_\sigma^2/2 + n_1kf_w^2 + i/2z, \quad (15)$$

$$C_2' = kf_\sigma^2/2 + n_2kf_w^2 - i/2z, \quad (16)$$

$$P' = 4C_1C_2 - k^2f_\sigma^4. \quad (17)$$

Equation (14) is the paraxial propagation analytical formula of the cross-spectral density matrix for a partially coherent flat-topped beam in free space.

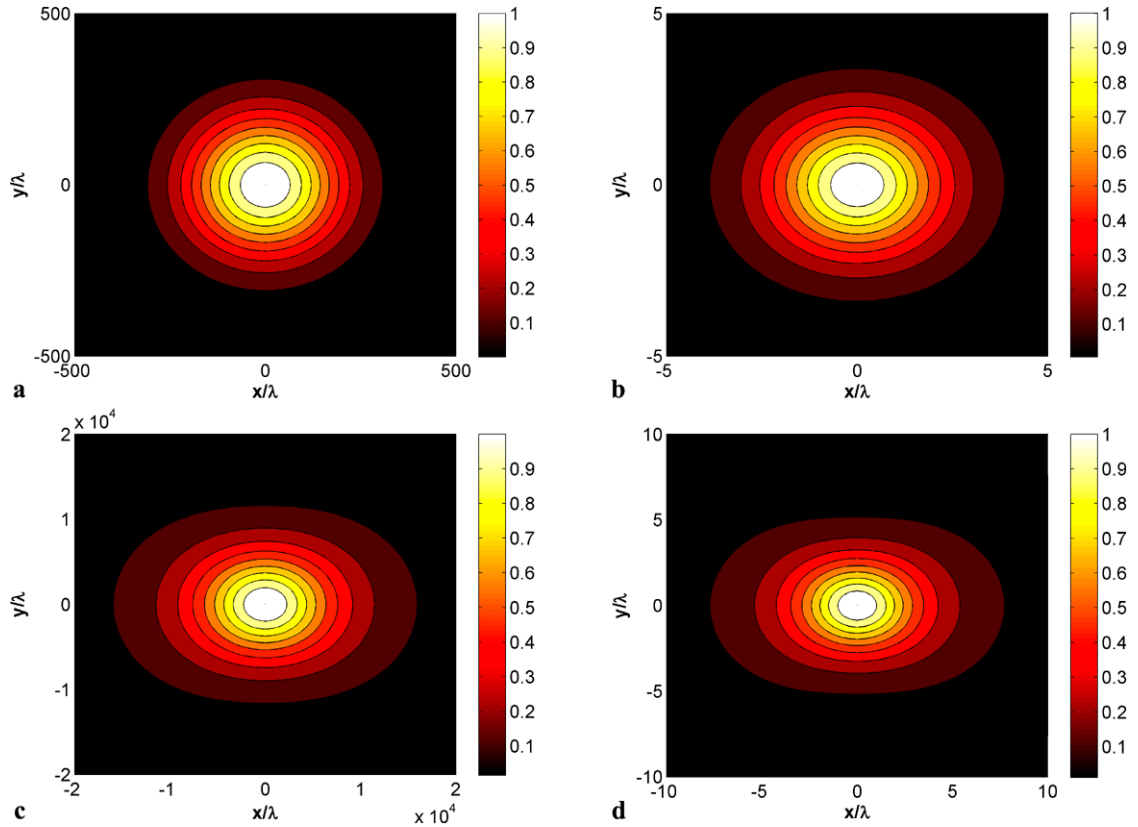

Fig. 3 The contour graphs of intensity distribution of a vectorial nonparaxial partially coherent flat-topped beam with $N = 20$ in the plane $z = 15z_R$ for different f_w and f_σ values. (**a**) $f_w = 0.01$, $f_\sigma = 0.01$; (**b**) $f_w = 0.5$, $f_\sigma = 0.01$; (**c**) $f_w = 0.01$, $f_\sigma = 0.5$; (**d**) $f_w = 0.5$, $f_\sigma = 0.5$

3 Numerical calculations and discussions

For illustrating the propagation properties of vectorial nonparaxial partially coherent flat-topped beams in free space and comparing the results with that of the paraxial case, numerical calculations were carried out by use of the formulae derived in Sect. 2. The normalized three-dimensional irradiance distributions of a partially coherent nonparaxial flat-topped beam with $N = 20$, $f_w = 0.01$, $f_\sigma = 0.01$ at various values of the propagation distance z are given in Fig. 1. The propagation distances are normalized to the Rayleigh distance z/z_R ($z_R = \pi w_0^2/\lambda$). One can see from Fig. 1 that the flat-topped profile of the vectorial nonparaxial partially coherent flat-topped beam gradually disappears during propagation and degenerates to the Gaussian distribution in the far field. In addition, numerical results show that this conversion from the flat-topped profile to the Gaussian profile occurs more rapidly during propagation for the beams with a large f_w or f_σ value.

Figure 2 gives the normalized irradiance distribution of a vectorial nonparaxial partially coherent flat-topped beam with $N = 20$ in the plane $z = 15z_R$ for different f_w and f_σ values. The corresponding paraxial results I_p and the z-component of the intensity I_z are plotted together for comparison. From Fig. 2(a) and (c), we see that when both parameters f_w and f_σ are very small, the result by using (6) coincides with that by using (12) quite well, so that for this case the paraxial approximation holds true and the z-component is very small and can be negligible. However, with the increasing f_w or f_σ, such as in Fig. 2(b) and (d), the difference between the nonparaxial results I and paraxial results I_p become obvious, the longitudinal component intensity becoming large and non-neglected. Therefore, from Fig. 2, we draw the conclusion that the paraxial approximation holds true for a vectorial partially coherent flat-topped beam when $f_w \leq 0.177$ and $f_\sigma \leq 0.18$, which is consistent with the previous results [14, 17]. It means that for the large values of $f_w > 0.177$ or $f_\sigma > 0.18$ the vectorial nonparaxial approach instead of the scalar paraxial one should be employed, and the vectorial nonparaxial behavior of the partially coherent flat-topped beam should be taken into consideration.

Figure 3 shows the contour graphs of the intensity distribution of a vectorial nonparaxial partially coherent flat-topped beam with $N = 20$ in the plane $z = 15z_R$ for different f_w and f_σ values. From Fig. 3(a), we can see that when both parameters f_w and f_σ are very small, the intensity distribution is axially rotational symmetry, which is coincident with the paraxial result. However, when f_w or f_σ

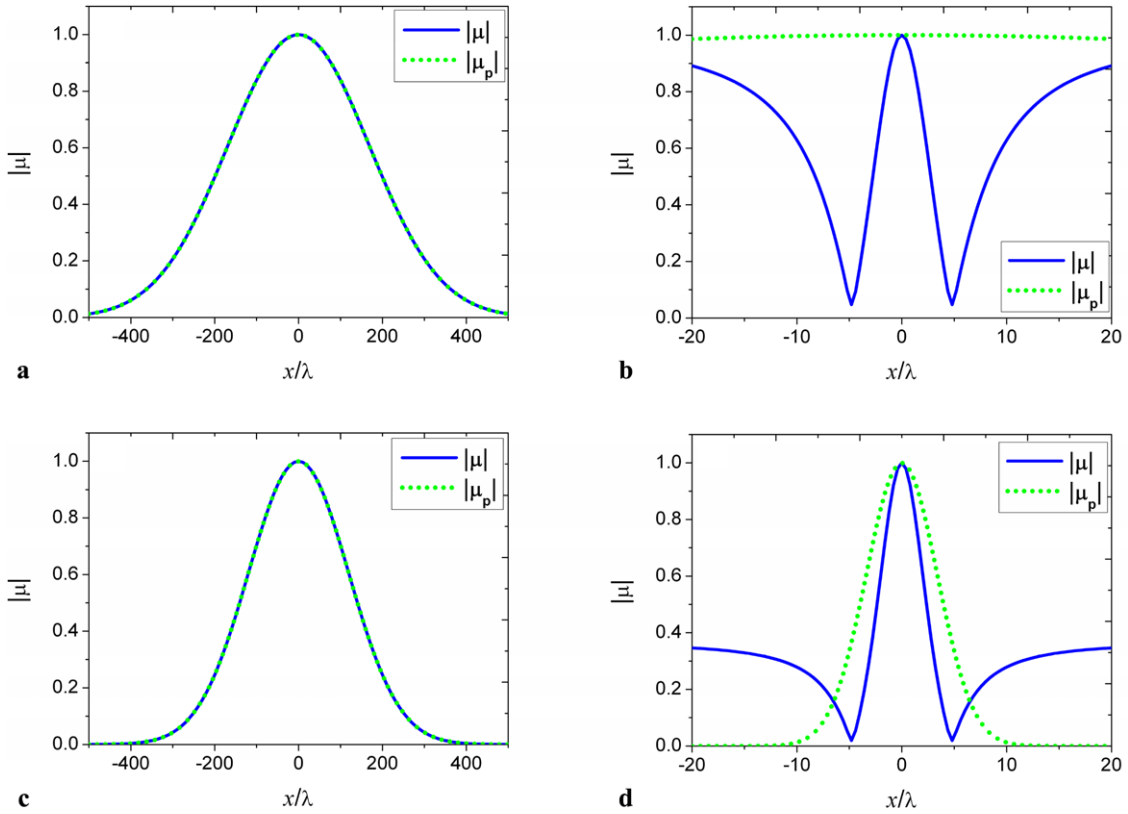

Fig. 4 The spectral degree of coherence of a vectorial nonparaxial GSM beam in the plane $z = 15z_R$ for different parameters f_w and f_σ. (**a**) $f_w = 0.01$, $f_\sigma = 0.01$; (**b**) $f_w = 0.5$, $f_\sigma = 0.01$; (**c**) $f_w = 0.01$, $f_\sigma = 0.5$; (**d**) $f_w = 0.5$, $f_\sigma = 0.5$

is not very small, shown as Fig. 3(b–d), the intensity distributions of partially coherent flat-topped beams lose their circular symmetry and become elliptically symmetric due to the longitudinal component intensity becoming large and non-neglected.

Figures 4–5 show the spectral degree of coherence of a vectorial nonparaxial partially coherent flat-topped beam with different beam orders in the plane $z = 15z_R$ for different parameters f_w and f_σ; $N = 1$ in Fig. 4 and $N = 20$ in Fig. 5. For convenience of comparison the corresponding paraxial results $|\mu_p|$ are also given in the figures. It can be seen from Figs. 4–5 that the transverse distribution of spectral degrees of coherence of partially coherent beams is dependent on the parameters f_w and f_σ. Comparing Fig. 4 with Fig. 5, we find the transverse distribution of spectral degrees of coherence for a vectorial nonparaxial partially coherent flat-topped beam with $N = 20$ are evidently different from those for a Gaussian Schell-model (GSM) beam ($N = 1$). The curves of spectral coherent degrees of a GSM beam are similar to a Gaussian profile distribution. For a partially coherent nonparaxial flat-topped beam, there are many sidelobes appearing in the curves of spectral degrees. The reason for this difference can be explained by the fact that a partially coherent flat-topped beam is not single mode; different modes evolve differently and overlap and interfere in the propagation. Furthermore, for the small value of $f_w = 0.01$ in Fig. 4(a) and (c) and Fig. 5(a) and (c), the $|\mu|$ of the nonparaxial beam coincide with those of the paraxial beam, thus the paraxial approximation of spectral coherent degrees is applicable. For the large value of $f_w = 0.5$ in Fig. 4(b) and (d) and Fig. 5(b) and (d), the discrepancy between the paraxial and nonparaxial results becomes noticeable, which makes the paraxial approximation of spectral coherent degrees inappropriate. It implies that the nonparaxiality of $|\mu|$ is dependent on parameter f_w and independent of parameter f_σ.

4 Concluding remarks

In conclusion, starting from the generalized vector Rayleigh diffraction integrals for the 3×3 cross-spectral density matrix of vectorial partially coherent beams, the analytical propagation expressions for the cross-spectral density matrix of the polarized vectorial nonparaxial partially coherent flat-topped beams have been derived. The corresponding paraxial approximation expressions have been dealt with as special cases of our general results. With the help of numerical calculations, the propagation properties of

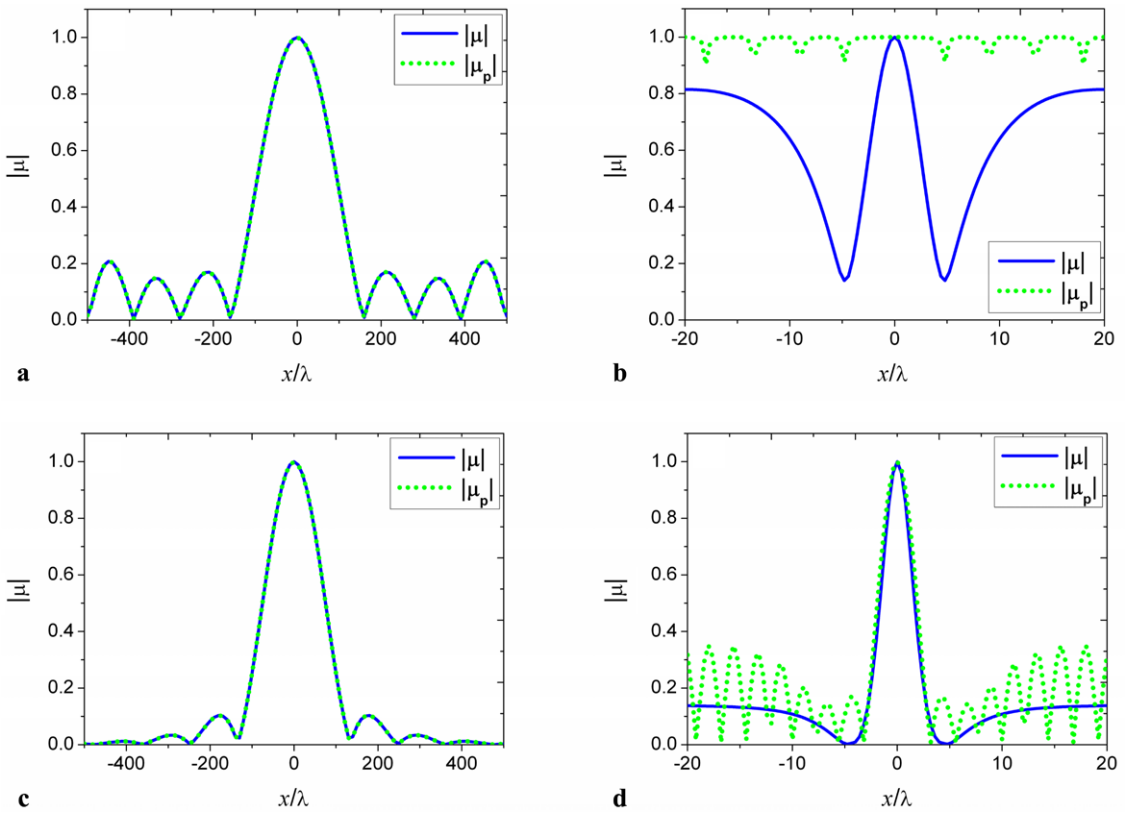

Fig. 5 The spectral degree of coherence of a vectorial nonparaxial partially coherent flat-topped beam with $N = 20$ in the plane $z = 15z_R$ for different parameters f_w and f_σ. (**a**) $f_w = 0.01$, $f_\sigma = 0.01$; (**b**) $f_w = 0.5$, $f_\sigma = 0.01$; (**c**) $f_w = 0.01$, $f_\sigma = 0.5$; (**d**) $f_w = 0.5$, $f_\sigma = 0.5$

the polarized vectorial nonparaxial partially coherent flat-topped beams have been studied and analyzed comparatively with the paraxial results. It has been found that the irradiance distribution of a vectorial nonparaxial partially coherent flat-topped beam cannot keep its shape invariant during propagation, and the spectral degrees of coherence are evidently different from those for a GSM beam. The nonparaxiality of partially coherent flat-topped beams for the irradiance distribution is determined by two key parameters f_w and f_σ, yet the nonparaxiality of the spectral degree of coherence is dependent on parameter f_w. The results afford an essential theoretical foundation of the applications of partially coherent flat-topped beams, and the method can be applied to study the nonparaxial propagation of other complicated partially coherent beams, such as partially coherent Hermite-Gaussian beams, partially coherent laser arrays, and partially coherent general-type beams.

Acknowledgements This work was supported by the Zhejiang Provincial Natural Science Foundation of China (Y606320, Y504111), Huzhou Civic Natural Science Fund of Zhejiang Province of China (2006YZ11) and National Natural Science Foundation of China (10874150). The authors are grateful to the reviewers for the many insightful comments that have improved this work.

Appendix: Derivation of the propagation formula of the cross-spectral density matrix (8)

Substituting from (7) into (5a), replacing R_m in the exponential term of (5) with (6) and the other terms with r_m, the cross-spectral density matrix element W_{xx} can be expressed as

$$
\begin{aligned}
&W_{xx}(\boldsymbol{\rho}_1, \boldsymbol{\rho}_2, z) \\
&= \left(\frac{z}{\lambda}\right)^2 \sum_{n_1=1}^{N} \sum_{n_2=2}^{N} \frac{(-1)^{n_1+n_2-2}}{N^2} \\
&\quad \times \binom{N}{n_1} \binom{N}{n_2} \frac{\exp[ik(r_2 - r_1)]}{r_1^2 r_2^2} \\
&\quad \times \int_{-\infty}^{\infty} \int_{-\infty}^{\infty} \exp\left[-C_1 x_{10}^2 + \left(\frac{ikx_1}{r_1} + \frac{x_{20}}{\sigma_0^2}\right) x_{10}\right] \\
&\quad \times \exp\left[-C_2 x_{20}^2 - \frac{ikx_2 x_{20}}{r_2}\right] \mathrm{d}x_{10}\, \mathrm{d}x_{20} \\
&\quad \times \int_{-\infty}^{\infty} \int_{-\infty}^{\infty} \exp\left[-C_1 y_{10}^2 + \left(\frac{iky_1}{r_1} + \frac{y_{20}}{\sigma_0^2}\right) y_{10}\right]
\end{aligned}
$$

$$\times \exp\left[-C_2 y_{20}^2 - \frac{iky_2 y_{20}}{r_2}\right] \mathrm{d}y_{10}\,\mathrm{d}y_{20}. \tag{A1}$$

Applying the following integral formula,

$$\int_{-\infty}^{\infty} \exp\left(-ax^2 - 2bx - c\right) x^R \,\mathrm{d}x$$
$$= \left(-\frac{b}{a}\right)^R \sqrt{\frac{\pi}{a}} \exp\left(\frac{b^2 - ac}{a}\right) \sum_{\varepsilon=0}^{[\frac{R}{2}]} \frac{\Gamma(2\varepsilon - R)}{\Gamma(-R)\varepsilon!} \left(\frac{a}{4b^2}\right)^{\varepsilon}, \tag{A2}$$

after performing tedious but straightforward integral calculations, we get

$$W_{xx}(\boldsymbol{\rho}_1, \boldsymbol{\rho}_2, z)$$
$$= \sum_{n_1=1}^{N} \sum_{n_2=2}^{N} \frac{(-1)^{n_1+n_2-2}}{N^2} \binom{N}{n_1} \binom{N}{n_2}$$
$$\times \frac{z^2 \exp[ik(r_2 - r_1)]}{r_1^2 r_2^2 P}$$
$$\times \exp\left\{-\frac{k}{P}\left[C_1 \frac{\boldsymbol{\rho}_2^2}{r_2^2} + C_2 \frac{\boldsymbol{\rho}_1^2}{r_1^2} - \frac{k f_\sigma^2 (x_1 x_2 + y_1 y_2)}{r_1 r_2}\right]\right\}. \tag{A3}$$

In the same way, the other cross-spectral density matrix elements can also be obtained.

References

1. M.S. Bowers, Opt. Lett. **19**, 1319 (1992)
2. F. Gori, Opt. Commun. **107**, 335 (1994)
3. Y. Li, Opt. Lett. **27**, 1007 (2002)
4. Z. Mei, D. Zhao, Appl. Opt. **44**, 1381 (2005)
5. Y. Cai, Q. Lin, J. Opt. A, Pure Appl. Opt. **6**, 390 (2004)
6. H.T. Eyyuboğlu, Ç. Arpali, Y. Baykal, Opt. Express **14**, 4196 (2006)
7. G. Wu, H. Guo, D. Deng, Opt. Commun. **260**, 687 (2006)
8. Y. Cai, S. He, J. Opt. Soc. Am. A **23**, 2623 (2006)
9. R. Borghi, M. Santarsiero, Opt. Lett. **23**, 313 (1998)
10. X. Ji, X. Chen, S. Chen, X. Li, B. Lü, J. Opt. Soc. Am. A **24**, 3554 (2007)
11. M. Alavinejad, B. Ghafary, D. Razzaghi, Opt. Commun. **281**, 2173 (2008)
12. F. Wang, Y. Cai, Opt. Lett. **33**, 1795 (2008)
13. Y. Cai, X. Lu, H.T. Eyyuboğlu, Y. Baykal, Opt. Commun. **281**, 3221 (2008)
14. S. Nemoto, Appl. Opt. **29**, 1940 (1990)
15. L. Mandel, E. Wolf, *Optical Coherence and Quantum Optics* (Cambridge University Press, London, 1995)
16. R.K. Luneburg, *Mathematical Theory of Optics* (University of California Press, Berkeley, 1966)
17. K. Duan, B. Lü, J. Opt. Soc. Am. A **21**, 1924 (2004)
18. Y. Qiu, A. Xu, J. Liu, J. Yan, J. Opt. A, Pure Appl. Opt. **10**, 1 (2008)
19. Z. Mei, D. Zhao, Opt. Express **15**, 11942 (2007)
20. A. Ciattoni, B. Crosignani, P.D. Porto, Opt. Commun. **202**, 17 (2002)